EPR Studies of Amine Radical Cations, Part 1: Thermal and Photoinduced Rearrangements of *n*-Alkylamine Radical Cations to their Distonic Forms in Low-Temperature Freon Matrices

I. Janovský,[a] W. Knolle,*[a] S. Naumov,[a] and F. Williams[b]

Abstract: The thermal and photochemical transformations of primary amine radical cations (*n*-propyl $\mathbf{1}^{\bullet+}$, *n*-butyl $\mathbf{5}^{\bullet+}$) generated radiolytically in freon matrices have been investigated by using low-temperature EPR spectroscopy. Assignment of the spectra was facilitated by parallel studies on the corresponding *N,N*-dideuterioamines. The identifications were supported by quantum chemical calculations on the geometry, electronic structure, hyperfine splitting constants and energy levels of the observed transient radical species. The rapid generation of the primary species by a short exposure (1–2 min) to electron-beam irradiation at 77 K allowed the thermal rearrangement of $\mathbf{1}^{\bullet+}$ to be monitored kinetically as a first-order reaction at 125–140 K by the growth in the well-resolved EPR signal of the distonic radical cation $^{\bullet}CH_2CH_2CH_2NH_3^+$. By comparison, the formation of the corresponding $^{\bullet}CH_2CH_2CH_2CH_2NH_3^+$ species from $\mathbf{5}^{\bullet+}$ is considerably more facile and already occurs within the short irradiation time. These results directly verify the intramolecular hydrogen-atom migration from carbon to nitrogen in these ionised amines, a reaction previously proposed to account for the fragmentation patterns observed in the mass spectrometry of these amines. The greater ease of the thermal rearrangement of $\mathbf{5}^{\bullet+}$ is in accordance with calculations on the barrier heights for these intramolecular 1,5- and 1,4-hydrogen shifts, the lower barrier for the former being associated with minimisation of the ring strain in a six-membered transition state. For $\mathbf{1}^{\bullet+}$, the 1,4-hydrogen shift is also brought about directly at 77 K by exposure to ~350 nm light, although there is also evidence for the 1,3-hydrogen shift requiring a higher energy. A more surprising result is the photochemical formation of the $H_2C{=}N^{\bullet}$ radical as a minor product under hard-matrix conditions in which diffusion is minimal. It is suggested that this occurs as a consequence of the β-fragmentation of $\mathbf{1}^{\bullet+}$ to the ethyl radical and the $CH_2{=}NH_2^+$ ion, followed by consecutive cage reactions of deprotonation and hydrogen transfer from the iminonium group. Additionally, secondary ion–molecule reactions were studied in $CFCl_2CF_2Cl$ under matrix conditions that allow diffusion. The propane-1-iminyl radical $CH_3CH_2CH{=}N^{\bullet}$ was detected at high concentrations of the *n*-propylamine substrate. Its formation is attributed to a modified reaction sequence in which $\mathbf{1}^{\bullet+}$ first undergoes a proton transfer within a cluster of amine molecules to yield the aminyl radical $CH_3CH_2CH_2N^{\bullet}H$. A subsequent disproportionation of these radicals can then yield the propane-1-imine precursor $CH_3CH_2CH{=}NH$, which is known to easily undergo hydrogen abstraction from the nitrogen atom. The corresponding butane-1-iminyl radical was also observed.

Keywords: amines · density functional calculations · EPR spectroscopy · matrix isolation · radical cations

Introduction

Amines are excellent electron donors on account of their low ionisation potentials;[1] therefore, it is not surprising that radical cations as diverse as those of *N,N,N′,N′*-tetramethyl-*p*-phenylenediamine (TMPD)[2] and 1,4-diazabicyclo[2.2.2]octane (DABCO)[3] are counted among the most stable forms of ionised organic molecules found in solution. Nevertheless, many radical cations derived from amines with diverse structures display significant reactivity, and their chemistry finds many useful applications. In fact, amines and their radical cations play a significant role in

[a] Dr. I. Janovský, Dr. W. Knolle, Dr. S. Naumov
Leibniz-Institut für Oberflächenmodifizierung (IOM)
Permoserstrasse 15, 04303 Leipzig (Germany)
Fax: (+49) 341-235-2584
E-mail: wolfgang.knolle@iom-leipzig.de

[b] Prof. F. Williams
Department of Chemistry, University of Tennessee
1420 Circle Drive, Knoxville, TN 37996-1600 (USA)
Fax: (+1) 865-974-3454

DOI: 10.1002/chem.200400401

many areas of polymer, biological and synthetic chemistry. Thus, in polymerisation reactions, the role of aliphatic amines as co-initiators in radiation- and UV-induced curing is well established,[4,5] the reaction mechanism consisting of a one-electron oxidation of the amine followed by proton transfer to generate a neutral radical. This is exemplified by the camphorquinone/amine initiator system widely used in practice for dental restorative materials.[6] In addition, so-called donor/acceptor systems that avoid the use of traditional photoinitiators have been developed.[7,8] While the formation of radical ion pairs again constitutes the first step towards the initiation of the polymerisation in such systems, the use of unsaturated amines as the donor component allows a fast rearrangement of the amine radical cation to occur, thereby reducing the probability of electron back-transfer and increasing the yield of initiating species. It is also noteworthy that the antioxidant action of HALS compounds (sterically hindered amine light stabilisers) is similarly based on electron transfer reactions and intermediate amine radical cations.[9]

The reactivity of amine radical cations is also of considerable biological significance.[10,11] Due to their formation as intermediates, they generally afford a relatively low-energy path for the metabolism of endogenous amines to the corresponding imines by enzymes such as monoamine oxidase.[10] The most likely mechanism for the one-electron oxidation occurs by means of electron transfer to the flavin group of the enzyme.[10d,e] Another facet of considerable biological interest concerns exogenous amines that function as enzyme inhibitors. These are often described rather dramatically as "suicide inactivators",[11a] and this terminology defines a class of enzyme inhibitors that are mechanism-based[10e] and become reactive only after interaction with the enzyme's active site. For certain of these amine inhibitors, the suicide action upon oxidation is considered to result from the rearrangement of the primarily formed nitrogen-centred aminium radical cation to a more potent chemical form, in which the biologically active species is thought to be a carbon-centred radical.[10d]

Aminium cation radicals[12] also serve as important intermediates in the Hofmann–Löffler–Freytag chain reaction[13] for the synthesis of pyrrolidine derivatives. Typically, these aminium species are generated by the oxidation of *N*-haloalkylamines under acid conditions,[12a,13d,13e] and the key propagation steps in the accepted mechanism of this overall reaction consist of an intramolecular 1,5-hydrogen transfer from the alkyl group to the nitrogen atom of the aminium radical cation,[13c] followed by reaction of the alkyl radical with the substrate by means of chlorine atom transfer. This results in a substituted ammonium ion pre-product, which, upon treatment with base, undergoes deprotonation and the elimination of hydrogen chloride with the generation of the desired substituted pyrrolidines.[13] Although detailed mass-spectrometric[14] and associated computational[15] studies of analogous abstraction reactions have been carried out on much simpler molecules, such as those of ionised alkylamines, even here the gas-phase processes are frequently accompanied by $-NH_3^+$ group migration and fragmentation,[14g–i] and there do not appear to be any previous investigations of such elementary reactions in the condensed phase.

Consequently, there is much interest in studying model reactions of amine radical cations under conditions in which the individual reaction steps can be isolated and well defined.[14i] Matrix isolation at low temperatures coupled with rapid generation of the ionised species by electron-beam irradiation and EPR detection provides an ideal method for following specific reaction pathways unhindered by competing processes. Here, in the first of two papers, we describe EPR, deuterium-labelling and computational studies on the intramolecular hydrogen-atom abstraction reactions that result in the rearrangement of the primary aminium radical cations of *n*-propylamine and *n*-butylamine to their distonic[16] forms. The photochemical reactivity of these primary radical cations has also been examined. A subsequent paper will report on the rearrangements of radical cations derived from several unsaturated amines, including those of allylamine, propargylamine and their derivatives.

Results and Discussion

EPR spectral assignments

n-Propylamine in the CF_3CCl_3 matrix: The EPR spectra of frozen solutions of *n*-propylamine ($PrNH_2$) in CF_3CCl_3 taken after irradiation at 77 K are shown in Figure 1. Initially, the spectrum observed in the dark at 77 K (Figure 1a), consists of a broad multiplet with a total spectral width of

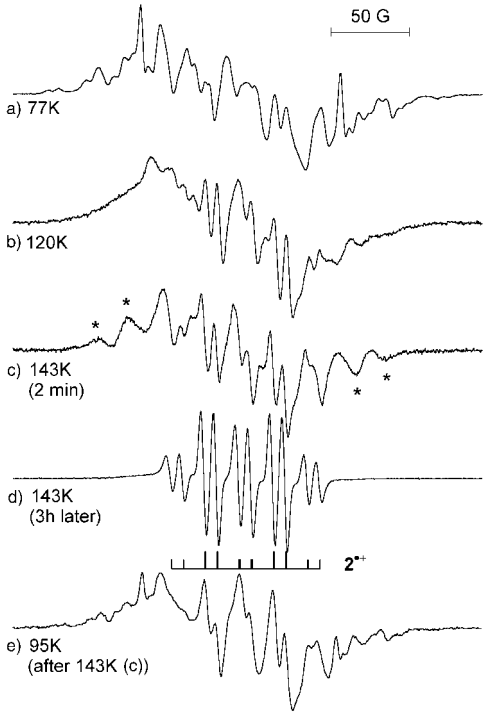

Figure 1. EPR spectra of a frozen solution (1:500) of *n*-propylamine in CF_3CCl_3 irradiated at 77 K and measured at the temperatures indicated. Spectrum c) obtained by quick warming to 143 K and spectrum e) by direct cooling down after spectrum c) was measured. Note that spectrum c) is plotted with seven-fold intensity in comparison to spectrum d). The hfc parameters used for stick plot of species $\mathbf{2}^{\bullet+}$ are *a*[G]: 44 (1H), 21.4 (2H) and 7.6 (1H).

approximately 245 G. The resolution of the pattern is slightly better at 95 K, and the spectral change is reversible in this low-temperature range. However, on increasing the temperature up to and above 120 K, a well-resolved spectrum grows in (Figure 1b–d and stick plot) with coupling constants of 44 G (1H), 21.4 G (2H) and 7.6 G (1H), as derived from the final 143 K spectrum. Although this transformation proceeds rather slowly at 140 K and takes three hours for completion, the process is quantitative with no loss of spin concentration (see Figure 8 below in kinetics section). Also, the broad outer features (marked with an asterisk in Figure 1c) are seen to disappear concomitantly with the formation of the secondary species. Confirmation that these signals belong to the primary species comes from the observation that the outermost features of the original spectrum are reproduced by cooling the sample back to 95 K immediately after a short (2 min) annealing at 140 K (Figure 1a and e). It should be noted that the overall splitting of ~185 G at 143 K is less than that observed at 77 K, an effect that is likely to result from a net reduction in the hyperfine anisotropy and from dynamic averaging of β-proton couplings (see later). Also, the outer features are not observed at 120 K (Figure 1b), possibly due to dynamic line broadening at this intermediate temperature.

To assist in the assignment of the initial and final spectra, *N,N*-dideuteriopropylamine ($PrND_2$) was synthesised for a comparative study. While its corresponding spectrum at 77 K (Figure 2a) is less resolved than that of the nondeuterated compound, there are some common features, such as the coincident positions of the sharper lines. The main difference lies in the overall spectral width, and although this is difficult to determine exactly, it is clear that the $PrND_2$ spectrum extends for only ~200 G, which is ~45 G narrower than that of the non-deuterated sample. However, this contraction is easily rationalised by assuming that the NH_2 protons each contribute an ~25–30 G (2H) splitting to the 77 K spectrum. Since the deuterium splittings are reduced by a factor of 6.54, they are not resolved due to the natural line width of ~5 G in the low-temperature matrix, and this effect contributes to a further broadening of the $PrND_2$ spectral lines. Hence, the deuteration not only eliminates the hydrogen splittings, but also increases the apparent line width, as observed.

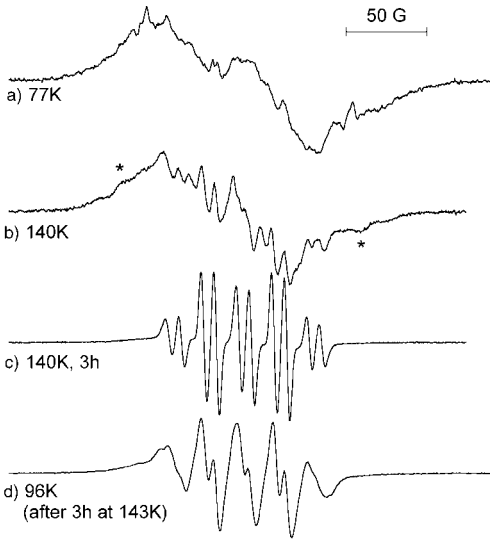

Figure 2. EPR spectra of a frozen solution (1:500) of [D_2]propylamine in CF_3CCl_3 irradiated at 77 K and measured at the temperatures indicated. Spectrum d) measured after complete annealing at 143 K.

Therefore, we assigned the initial 77 K spectrum to the parent radical cation **1**$^{\bullet+}$ of *n*-propylamine. Quantum chemical calculations (Tables 1 and 2) are consistent with the above estimates for the hfs of the NH_2 protons. Moreover, the values are in good agreement with the literature data for other alkyl amines (~22–23 G).[17] According to the

Table 1. Spin density (ρ), Mullikan charge distribution (q) and coupling constants (a[G]) for isomeric amine radical cations and radicals, calculated with B3LYP/6–31G(d). Data are given for the most stable conformer. Relative stability ΔE[kJ mol^{-1}] (including zero point vibrational energy) is given with respect to the most stable isomer.

	1a$^{\bullet+}$	**1b**$^{\bullet+}$	**2**$^{\bullet+}$	**3**$^{\bullet+}$	**4**$^{\bullet+}$	**7**$^{\bullet}$	**8**$^{\bullet}$	**9**$^{\bullet}$	**10**$^{\bullet}$
	$\bullet^{+}NH_2$		$\bullet\oplus NH_3$	$\bullet\oplus NH_3$	$\bullet\oplus NH_3$	$\bullet NH$	$\bullet NH_2$	$\bullet NH_2$	$\bullet NH_2$
$\Delta E(E_0+ZP)$	0.0	+10.3	−4.8	−22.1	+7.5	+18.9	0.0	+27.3	+44.4
ρ(N)	**0.746**	**0.877**	0.009	0.048	−0.047	**0.987**	0.151	0.082	0.003
ρ(C1)	0.026	−0.005	0.020	−0.016	**1.019**	−0.066	**0.859**	−0.059	0.014
ρ(C2)	0.186	−0.003	−0.063	**0.951**	−0.070	0.002	−0.057	**0.999**	−0.077
ρ(C3)	0.034	0.001	**1.040**	−0.069	0.020	0.000	0.006	−0.079	**1.087**
q(N)	0.390	0.442	0.557	0.547	0.573	−0.163	−0.070	−0.111	−0.131
q(C1)	0.309	0.359	0.265	0.239	0.234	0.123	0.092	0.118	0.123
q(C2)	0.142	0.088	0.125	0.113	0.118	0.057	−0.008	0.012	0.040
q(C3)	0.158	0.111	0.053	0.101	0.075	0.018	−0.013	−0.019	−0.032
a(N)	13.6	16.2	1.1	21.1[a]	−2.0	13.6	6.2	1.9	−0.3
a(H,N)	−19.5(2H)	−23.2(2H)	−0.6(3H)	0.4(3H)	17.7(3H)	−21.8	4.0/5.3	−2.4(2H)	0.1
a(H,C1)	18.9/18.9	85.2(2H)	−0.7(2H)	6.5/7.9	−23.2	46.0(2H)	−11.4	6.9/4.9	0.7(2H)
a(H,C2)	−2.8(2H)	2.4(2H)	45.5/3.4	−22.8	55.2/7.3	−0.5(2H)	10.4/35.4	−22.3	51.1/13.2
a(H,C3)	7.8(3H)	0.2(3H)	−19.9/−22.8	27.7(3H)	−0.5(3H)	0.1(3H)	−0.5(3H)	24.1(3H)	23.9(2H)

[a] Due to strong through-space spin polarisation.

Table 2. Spin density (ρ), Mullikan charge distribution (q) and coupling constants (a[G]) for isomeric amine radical cations and radicals, calculated with BH&HLYP/6–31G(d). Data are given for the most stable conformer. Relative stability ΔE[kJ mol^{-1}] (including zero point vibrational energy) is given with respect to the most stable isomer.

	1a$^{\bullet+}$	**1b**$^{\bullet+}$	**2**$^{\bullet+}$	**3**$^{\bullet+}$	**4**$^{\bullet+}$	**7**$^{\bullet}$	**8**$^{\bullet}$	**9**$^{\bullet}$	**10**$^{\bullet}$
	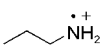		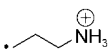	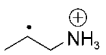	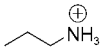	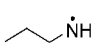	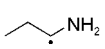	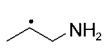	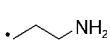
$\Delta E(E_0+ZP)$	0.0	+2.7	−15.5	−29.9	−3.4	+12.1	0.0	+24.9	+38.6
ρ(N)	**0.902**	**0.980**	0.009	0.042	−0.058	**1.020**	0.124	0.067	0.002
ρ(C1)	−0.036	−0.051	0.020	−0.047	**1.063**	−0.088	**0.914**	−0.079	0.015
ρ(C2)	0.138	0.000	−0.083	**1.027**	−0.092	0.004	−0.075	**1.060**	−0.099
ρ(C3)	0.024	0.000	**1.087**	−0.094	0.020	−0.001	0.007	−0.101	**1.128**
q(N)	0.450	0.476	0.559	0.551	0.574	−0.169	−0.094	−0.134	−0.148
q(C1)	0.301	0.344	0.276	0.259	0.247	0.132	0.112	0.142	0.141
q(C2)	0.113	0.070	0.116	0.093	0.108	0.057	−0.009	0.006	0.034
q(C3)	0.136	0.110	0.049	0.095	0.071	−0.015	−0.009	−0.014	−0.027
a(N)	20.5	22.0	0.7	16.2[a]	−2.4	17.3	5.6	2.88	−0.3
a(H,N)	−27.0(2H)	−29.0(2H)	−0.9(3H)	0.1(3H)	18.0(3H)	−25.3	4.7/3.1	−2.4(2H)	0.1/−0.1
a(H,C1)	18.5(2H)	68.6(2H)	−0.8/−0.8	7.0/8.1	−27.2	43.6(2H)	−14.8	7.8/5.8	−0.9(2H)
a(H,C2)	−3.6(2H)	0.1(2H)	45.7/4.1	−25.8	52.5/7.2	−0.7(2H)	11.2/36.0	−26.3	50.1/13.3
a(H,C3)	3.2(3H)	0.3(3H)	−23.6/−26.7	27.5(3H)	−0.7(3H)	0.1(3H)	−0.6(3H)	24.4(3H)	28.0(2H)

[a] Due to strong through-space spin polarisation.

given empirical relationship between hydrogen and nitrogen couplings in nitrogen-centred radicals, an a_{iso}(N) value of ~18 G can thus be expected. The literature[18] suggests that the corresponding anisotropic components of the nitrogen hfs tensor would then be in the region of $A_{\parallel}$(N) = 45 G and $A_{\perp}$(N) = 5 G. The determination of the β-proton couplings is less straightforward, as the primary radical cation spectrum at 77 K shows anisotropic contributions, probably due to both the nitrogen atoms, as mentioned above, as well as the α-protons on the amino group. However, even taking into account this anisotropy, it is clear that the total spectral width can only be explained by a geometry resulting in large β-proton couplings. Furthermore, the observation of the common, sharp features for $PrNH_2$ and $PrND_2$ (Figures 1a and 2a) can be rationalised by assuming that they result from the $M_I = 0$ transitions for the two amino protons/deuterons, in which case they correspond to only β-proton couplings. Also, it may be noted that since these sharp lines are unaffected by the nitrogen anisotropy, they presumably belong to the $M_I(^{14}N) = 0$ spectral components. From the distance between the outer sharp lines, a sum of β-proton couplings (at 77 K) in the region of 130 G is estimated. At 143 K, an estimate of the β-proton hfc (hyperfine coupling constant) can be made from the difference between the spectrum taken immediately after warming to 143 K (Figure 1c) and that recorded three hours later (Figure 1d). The multiplet spectrum obtained was simulated satisfactorily (in an isotropic powder approximation) with couplings of 43 G ($2H_\beta$), 24.6 G ($2H_\alpha$(N)) and 20.1 G (N_{iso}). Interestingly, two conformers (**1a**$^{\bullet+}$ and **1b**$^{\bullet+}$) are calculated (Scheme 1), differing mainly in the orientation of the π-radical at the (nearly planar) NH_2 group with respect to the neighbouring methylene group; the eclipsed conformer (**1b**$^{\bullet+}$) with the large β-H couplings has a slightly higher heat of formation

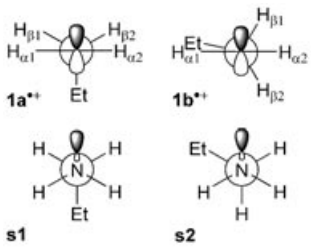

Scheme 1.

(+10.3 and +2.7 kJ mol^{-1} by B3LYP and BH&HLYP, respectively, see Tables 1 and 2).

Reconciliation of the experimental results above with the calculations (Tables 1 and 2) suggests that at 143 K, averaging of the β-proton hfc may occur either due to interconversion of the two conformers or by nearly complete rotational averaging. However, in order to account for the reduced spectral width at 143 K (Figure 1c, asterisk) relative to 77 K (Figure 1a) as well as the large β-couplings associated with the 77 K spectrum, this explanation would require the eclipsed conformer **1b**$^{\bullet+}$ with the larger β-proton hfc to be the more stable form, reversing the order predicted by the calculations. As the calculated energy difference between **1a**$^{\bullet+}$ and **1b**$^{\bullet+}$ is very small, the reversed order could be a result of interaction with the matrix. It is also interesting to consider the singlet ground-state geometry of the neutral molecule. Two real conformers **s1** and **s2** (no negative frequencies in this case) are calculated (Scheme 1), showing the expected high pyramidality on nitrogen with the lone-pair orbital positioned anti and gauche, respectively, to the ethyl group. In comparison with the conformers of the radical cation, the neutral ground-state conformers are separated by a much higher energy difference (ca. 40 kJ mol^{-1}). The more stable conformer **s2** clearly exhibits a more favourable

geometry for the formation of the radical cation $\mathbf{1b}^{\bullet+}$, which could explain further the initial observation of $\mathbf{1b}^{\bullet+}$ after ionisation.

Annealing the $PrND_2$ sample above 110 K leads to the appearance of the same secondary spectrum as in the case of $PrNH_2$. The transformation at 140 K proceeds at a similar rate to that of $PrNH_2$, the broad outer features (marked with asterisks in Figure 2b) again decaying concomitantly with the formation of the secondary spectrum. As expected from the results at 77 K (vide supra), the overall spectral width defined by these features at 120–140 K is again some 30–40 G narrower than that in the corresponding $PrNH_2$ case. Therefore, although the primary $PrND_2$ spectrum is subject to a greater congestion of lines, it can be assigned to the parent radical cation by analogy to the results for $PrNH_2$. Even more significantly for these two systems, the spectra that grow in at $\approx$140 K are seen to be completely identical (Figures 1d and 2c). Thus, in view of the same splitting constants for these spectra and the absence of any deuterium effect on the rate of the transformation (Figure 8 below), the only reasonable assignment for the secondary radical is to the distonic radical cation $\mathbf{2}^{\bullet+}$ and its deuterated analogue (Scheme 2), formed in each case by the intramolecular 1,4-hydrogen-atom transfer from the terminal methyl group to the ionised amine group (reaction enthalpies and activation energies are given in Figure 3).

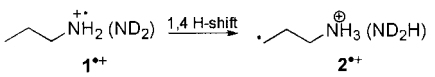

Scheme 2.

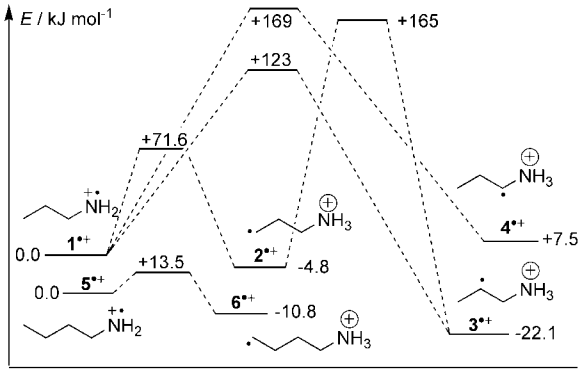

Figure 3. Energy diagram for transformations of propyl- and butylamine radical cations.

The assignment is strongly supported by the quantum chemical calculations for $\mathbf{2}^{\bullet+}$, as the hfc constants calculated (Tables 1 and 2) agree well with the experimental values given in the caption to Figure 1. (Note that the hfc's are calculated for the most stable conformer, which has indeed a geometry similar to the transition-state geometry $\mathbf{1}^{\bullet+} \rightarrow \mathbf{2}^{\bullet+}$.)

n-Propylamine in the CF_3CCl_3 matrix—photobleaching experiments: To check the stability of the primary radical cation to excitation, photobleaching experiments were performed. Whereas illumination of the samples at 77 K with light of $\lambda > 400$ nm had no effect, a transformation was induced on using UV light in the range 350–400 nm (below 350 nm the light is not transmitted due to the use of a glass sample cell), leading to essentially the same spectral pattern for both $PrNH_2$ and $PrND_2$ (Figure 4a and b). The spectral changes observed upon warming (Figure 4c) are completely reversible and are mainly due to improved resolution resulting from the smaller intrinsic line width at the higher temperatures. By comparison with the spectra of the distonic species $\mathbf{2}^{\bullet+}$ recorded at 140 and 95 K (Figure 2c and d), one can deduce that the spectra after photobleaching result from the overlapping patterns of several species, one of which is easily identified as species $\mathbf{2}^{\bullet+}$. It should be noted that distonic isomer $\mathbf{2}^{\bullet+}$ is produced directly at 77 K upon photobleaching, its three main lines dominating the central part of the spectrum at low temperature (95 K, see Figure 4a), and no further increase in intensity is observed upon raising the temperature to 143 K.

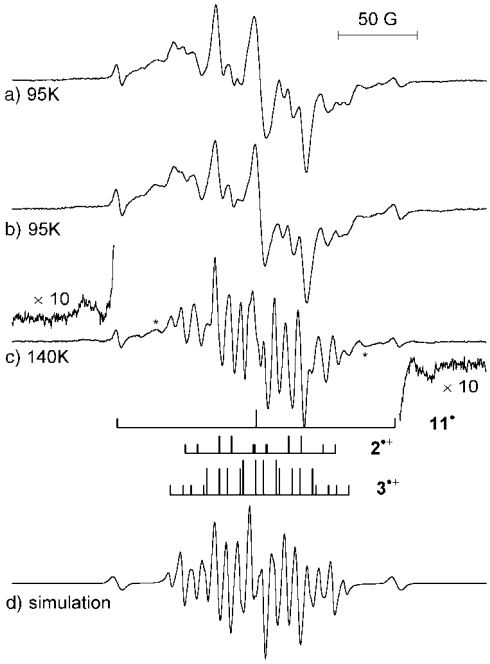

Figure 4. EPR spectra after photobleaching ($\lambda \approx$ 350–400 nm) at 77 K of frozen solutions (1:500) of propylamine (a and c) and [D_2]propylamine (b) in CF_3CCl_3, irradiated at 77 K and measured at the temperatures indicated. The hfc parameters used for the stick plots and for the simulation (d) are given in the text. (Relative concentrations of $\mathbf{11}^{\bullet}$, $\mathbf{2}^{\bullet+}$ and $\mathbf{3}^{\bullet+}$ are 5%, 25% and 70%, respectively.)

The remaining spectrum was more difficult to assign. The outer lines with a spacing of about 175 G actually belong to a triplet spectrum marked $\mathbf{11}^{\bullet}$ in Figure 4. This triplet is also formed to a certain extent if the sample is kept at 140 K until the transformation from $\mathbf{1}^{\bullet+}$ into $\mathbf{2}^{\bullet+}$ is completed (without a preceding illumination), and then subjected to photobleaching. The difference between the spectra taken at 140 K before and after photobleaching shows a 1:2:1 triplet

of narrow lines and a coupling constant of 87.8 G, each of these lines being accompanied by broad wing features (Figure 5). At first sight, the large coupling constant would seem to indicate a radical of the $^{\bullet}CF_2X$ type containing 2 α-fluorine atoms, and an almost identical *a*(2F) coupling of

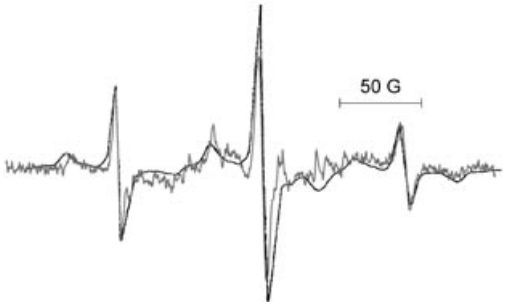

Figure 5. EPR spectrum of methyleneiminyl radical **11**$^{\bullet}$ obtained at 143 K in the CF_3CCl_3 matrix (noisy grey line, for experimental details see text) and at 77 K after photobleaching of formaldazine[21d] (smooth black line, reproduced with permission from *J. Phys. Chem.* **1971**, *75*, 164. Copyright by the American Chemical Society).

87.6 G was found for the $CF_3CF_2^{\bullet}$ radical in solution.[19] However, an assignment of this signal carrier to the corresponding $CCl_3CF_2^{\bullet}$ species formed from CF_3CCl_3 seems improbable, given that the spectra of neutral freon radicals with isotropic line shapes are usually observed only well above the matrix softening points (150 K for CF_3CCl_3).[20] Considering that the sharp lines (2 G line widths) of the triplet are observed even at temperatures well below 143 K (77–95 K, Figure 4a and b), and that the signals from **11**$^{\bullet}$ are only detected in experiments when the *n*-propylamines are present in the matrix, a more reasonable assignment is to the small methyleneiminyl radical $H_2C{=}N^{\bullet}$, for which *a*(2H) is reported to be in the range 87–91 G, depending on the matrix.[21] Moreover, the additional wing features present in the spectrum (Figure 4c, ×10) can be interpreted as originating from the anisotropic coupling of around 30 G to the nitrogen atom. Indeed, confirmation of this assignment is provided by the fact that the difference spectrum (see Figure 5) is virtually identical to that of the $H_2C{=}N^{\bullet}$ radical derived directly by the photolysis of formaldazine in a rigid matrix at 77 K.[21d] The contribution of **11**$^{\bullet}$ to the total spin population is in the order of 5% or less, and, therefore, it is a minor product in these transformations of the propylamine radical cations. A possible pathway for its formation is discussed below.

Having identified two species present in the spectrum of Figure 4c, namely **2**$^{\bullet+}$ and **11**$^{\bullet}$, the remaining spectral features are spaced by 20–25 G splittings with an overall spectral width of 125 G. Assuming that only intramolecular rearrangement reactions are possible in CF_3CCl_3 below 145 K, calculations suggest that the distonic isomer **3**$^{\bullet+}$ of the radical cation, formed by 1,3-hydrogen transfer from the C2 atom to the amino group, is favoured over isomer **4**$^{\bullet+}$, formed by 1,2-hydrogen transfer from C1 (see Scheme 3 and the energy diagram in Figure 3).

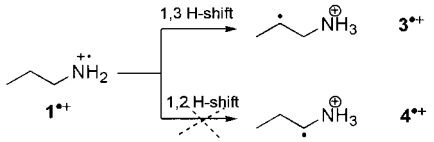

Scheme 3.

The exclusion of species **4**$^{\bullet+}$ is supported further by the observation that deuteration of the amino group in the β-position to C1 did not change the observed spectrum. Coupling constants *a*(H) of 24 (3H, CH_3), 21 (H_α) and 11.9/6.9 G (2H_β) were derived for **3**$^{\bullet+}$ by taking the calculated values given in Tables 1 and 2 as a starting point for the simulation. It should be noted that an unexpectedly high nitrogen coupling of 21 G is calculated as a result of a strong through-space spin polarisation in this isomer. Some weak wing components (see Figure 4c, asterisk) that are not covered by the simulation (Figure 4d) can be assigned tentatively to this nitrogen coupling.

Considering the possibility of deprotonation of the primary radical cation **1**$^{\bullet+}$, the α-aminoalkyl radical **8**$^{\bullet}$ would be superior over the nitrogen-centred radical **7**$^{\bullet}$ and the other two carbon-centred radicals **9**$^{\bullet}$ and **10**$^{\bullet}$ by +18.9, +27.3 and +44.4 kJ mol^{-1}, respectively (see Table 1). However, if the energetically preferred radical **8**$^{\bullet}$ or even the less stable amino radical **7**$^{\bullet}$ would be formed, deuteration of the amino group should affect the observed EPR spectrum. However, this is not the case. Also, deprotonation in freon matrix usually occurs only if a proton acceptor (i.e., another solute molecule) is available. Even at the rather high concentration of 1:20 no significant differences are observed. Therefore, radical formation by deprotonation can be ruled out in the "hard" freon.

Another possible reaction channel of the radical cation **1**$^{\bullet+}$ will now be discussed. The β-fragmentation reaction (also known as the α-cleavage of a C–C bond in the mass spectrometry literature[14]) is found to be a main reaction channel at high ionisation energies in the gas phase for primary *n*-alkyl amines, and would lead in the case of **1**$^{\bullet+}$ to the ethyl radical and the $CH_2{=}NH_2^+$ ion. The dissociation energy is estimated (in vacuo) to be rather low, only +20 to 40 kJ mol^{-1}; however, the separation of both fragments is considered to be unlikely in the frozen matrix. Even if the remaining spectrum can be fitted well with a set of two and three magnetically equivalent protons, the coupling constants of 21 G (2H) and 23 G (3H), respectively, obtained in that case do not agree with the data for the ethyl radical. In particular, the value for the methyl protons of the ethyl radical is much larger (26.8 G (3H, CH_3)).[22] Although this excludes the ethyl radical as a contributor to the observed spectrum, the ethyl radical produced by such a β-fragmentation reaction in the solid state may readily abstract a hydrogen atom from the geminate $CH_2{=}NH_2^+$ ion or its conjugate base, $CH_2{=}NH$. Quantum chemical calculations show that whereas the former reaction is unlikely ($\Delta H \sim$ +120 kJ mol^{-1}), the latter would be possible due to an enthalpy change of −71 kJ mol^{-1}. In this case, hydrogen abstraction from the nitrogen leads to the methyleneiminyl

radical $CH_2{=}N^{\bullet}$, which, as mentioned earlier, is the signal carrier responsible for the triplet spectrum labelled **11**$^{\bullet}$. The whole reaction sequence is considered to proceed under cage-like conditions and may be written formally as shown in Scheme 4, in which the deprotonation step probably involves transfer to a negatively charged matrix species like Cl^-.

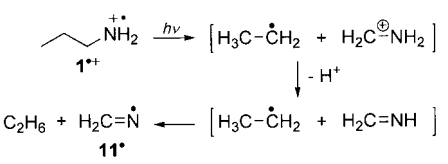

Scheme 4.

n-Propylamine in the $CFCl_2CF_2Cl$ matrix: The EPR spectra of irradiated frozen solutions (1:500) of $PrNH_2$ and $PrND_2$ in $CFCl_2CF_2Cl$ taken at 77 K and 95 K are broad and relatively structureless. The width of the spectra of both amines is similar to that in CF_3CCl_3 matrix and it is likely that the primary radical cation **1**$^{\bullet+}$ is observed in F-113 as well. At the low concentration of 1:500 a temperature increase to ~ 100 K leads to some irreversible changes in the spectra. Although the spectra remain relatively unresolved, the new features do not correspond to the splittings of the distonic species **2**$^{\bullet+}$ observed in CF_3CCl_3. In contrast to the latter matrix, F-113 is commonly used to study ion–molecule reactions,[20c] the onset of these reactions being around 105 K.

To check if the observed changes are due to such ion–molecule reactions, concentrated solutions (1:10) were investigated. As a result, the EPR patterns that appeared at ~ 100 K at the lower concentration now already dominate the spectra at 77–95 K (Figure 6a and b). Comparison of the spectra of $PrND_2$ and $PrNH_2$ clearly shows the loss of one

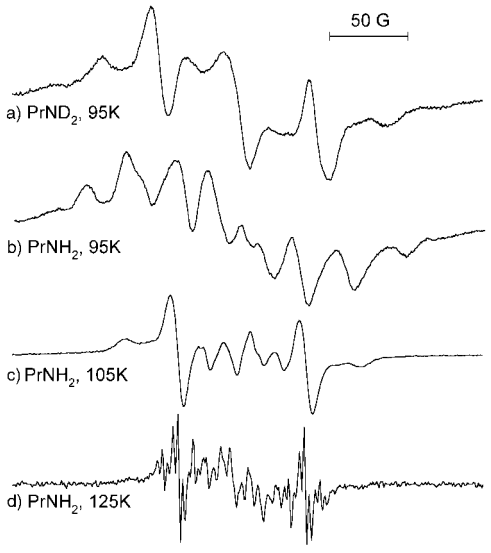

Figure 6. EPR spectra of frozen solutions (1:10) of $PrND_2$ (a) and $PrNH_2$ (b–d) in F-113 irradiated at 77 K and measured at temperatures indicated.

proton coupling of 28 G upon exchange of the amine protons. Therefore, the most likely explanation for the radical structure in both cases is the aminyl radical **7**$^{\bullet}$ $CH_3CH_2CH_2N^{\bullet}H$ or its deuterated analogue $CH_3CH_2CH_2N^{\bullet}D$, in which the deuterium splitting is unresolved due to the natural line width in this matrix. As for the preceding radical cation **1**$^{\bullet+}$ (see above), radical **7**$^{\bullet}$ retains a conformation with two large β-proton couplings of approximately 53 G each. The additional nitrogen splitting has an $a_{iso}(N)$ value of approximately 22 G, but the remaining anisotropy is clear (Figure 6a). From the EPR spectra it is impossible to decide if the radical cation **1**$^{\bullet+}$ deprotonates or abstracts a hydrogen atom from a neutral molecule. In either case, radical **7**$^{\bullet}$ is formed together with the ammonium-type cation $R{-}NH_3^+$ (Scheme 5). We propose that at

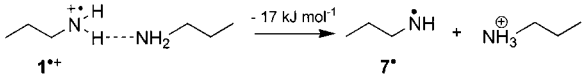

Scheme 5.

high concentration the amine does not dissolve in freon to give isolated single molecules, but associates through hydrogen bonding to give dimeric or higher clusters (the stabilisation energy of a hydrogen-bonded dimer is calculated to be $-20.8\,kJ\,mol^{-1}$), in which deprotonation/abstraction may readily occur at 77 K; at lower concentration the reaction occurs after softening of the matrix. The preferential formation of the aminyl radical **7**$^{\bullet}$, which is energetically less stable than the α-amino alkyl radical **8**$^{\bullet}$ by $18.9\,kJ\,mol^{-1}$, is also explained well by the hydrogen bonding between the amino groups.

By increasing the temperature to 105 K in the case of the high concentration, a doublet spectrum (ca. 80 G) appears (Figure 6c), showing an additional anisotropic nitrogen splitting, similar to that observed for the aminyl radical **7**$^{\bullet}$ (Figure 6a). At low concentration this doublet appears after warming the sample to 115–120 K. The spectrum is quite well resolved at 125 K (Figure 6d, note that the central part of the spectrum contains lines from another species) and coupling constants of 80.5 G ($1\,H_\beta$), 9.9 G ($1\,N_{iso}$) and 2.8 G ($2\,H_\gamma$) are derived. The values agree exactly with the data for the propane-1-iminyl radical **12**$^{\bullet}$ ($CH_3CH_2CH{=}N^{\bullet}$), observed in the case of cyclopropylamine in the same matrix after ring opening and subsequent hydrogen transfer.[23] The observation of radical **12**$^{\bullet}$ seems to be surprising at first sight, but the assignment can be regarded as definitive. A possible (and probably the most likely) explanation is based on two further reaction steps involving radicals and/or the primary radical cations. Considering the termination reaction of two aminyl radicals **7**$^{\bullet}$, quantum chemical calculations predict the disproportionation reaction leading to the imine/amine pair to be superior to the recombination reaction ($\Delta H = -330$ and $-250\,kJ\,mol^{-1}$, respectively). The subsequent hydrogen abstraction from the imine by an aminyl radical **7**$^{\bullet}$ is exothermic by $-91\,kJ\,mol^{-1}$ and leads to **12**$^{\bullet}$ (Scheme 6). The latter is also formed in the case of $PrND_2$, although in much smaller amounts, pointing to an isotope effect in these reaction steps.

Scheme 6.

Replacing one aminyl radical by the primary radical cation $\mathbf{1}^{\bullet+}$ in each of the above equations results in calculated reaction enthalpies of -313 and $-77\,kJ\,mol^{-1}$ that are of comparable exothermicity, the driving force arising from the formation of the highly stabilised ammonium-type RNH_3^+ ion. The pronounced formation of the iminyl radical already at 105 K at high concentration is best explained if one assumes the presence of not only dimeric but also higher clusters of amine molecules, all associated through hydrogen bonding in a head-to-head arrangement of the amine groups.

n-Butylamine in the CF_3CCl_3 and $CFCl_2CF_2Cl$ matrices: In the transformations of the primary radical cations of alkylamines carried out by mass-spectrometric studies, it has been shown that hydrogen transfer to the amino group is facilitated for alkyl chains containing at least four carbon atoms.[14–16] For this reason, *n*-butylamine ($BuNH_2$) and partially deuterated [D_2]*n*-butylamine ($BuND_2$) were investigated in order to evaluate the effect of chain length on the efficacy of the rearrangement. In both cases, exactly the same spectra are observed in CF_3CCl_3 already at 77 K, and these do not change upon increasing the temperature to the matrix softening point of 143 K (Figure 7a), except for some

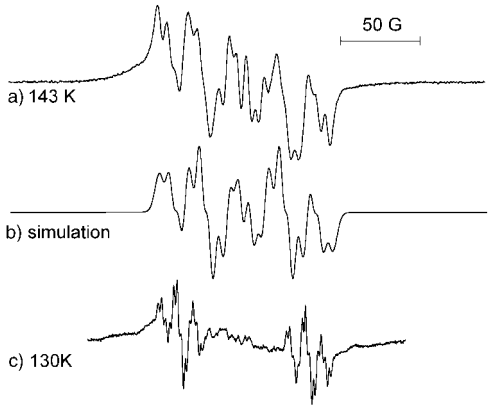

Figure 7. EPR spectra of frozen butylamine/freon solutions, irradiated at 77 K and measured at the temperatures indicated. a) 1:500, CF_3CCl_3; c) 1:9, $CFCl_2CF_2Cl$. The hfc parameters used for simulation (b) are *a*/G: 50 (1H), 19.6 (2H), 6 (1H) and 4.9 (N_{iso}); these parameters are assigned to the distonic radical cation $\mathbf{6}^{\bullet+}$ formed from the *n*-butylamine radical cation $\mathbf{5}^{\bullet+}$ by an intramolecular 1,5-hydrogen shift (see Figure 3).

line width narrowing in the latter case. The spectrum is well analysed as a doublet ($a(1H) = 50$ G) of triplets ($a(2H) = 19.6$ G) with further small splittings in the order of 4–6 G. The best simulation is achieved by using an additional proton coupling of $a(1H) = 6$ G and an isotropic nitrogen coupling of $a(N) = 4.9$ G (Figure 7b). The spectrum can be straightforwardly assigned to the distonic radical cation $\mathbf{6}^{\bullet+}$ (see Figure 3), with 2α- and 2β-protons (19.6 G ($2H_\alpha$) and 50/6 G ($2H_\beta$)). The assignment is supported by the stability of the species under different experimental conditions and the absence of any effect from deuteration. It also agrees well with quantum chemical calculations for the hyperfine couplings in species $\mathbf{6}^{\bullet+}$. Additionally, the calculated activation energy of the six-membered transition state is smaller and the reaction enthalpy larger than in the case of propylamine with a five-membered transition state (Figure 3). Thus, it is hardly surprising that at 77 K, this hydrogen transfer in the butylamine radical cation $\mathbf{5}^{\bullet+}$ already occurs too rapidly to be observed, whereas for propylamine, additional energy in the form of a temperature increase or UV illumination is needed to drive the reaction.

Irradiation of $BuNH_2$ and $BuND_2$ in the $CFCl_2CF_2Cl$ matrix at a concentration of 1:500 leads to the same spectrum (no effect of deuteration) as that observed in CF_3CCl_3. This signal is stable up to 110 K and despite some broadening similar to that encountered in the CF_3CCl_3 matrix, the spectrum can be confidently assigned to the distonic species $\mathbf{6}^{\bullet+}$. Even at the rather high concentration of 1:9, $\mathbf{6}^{\bullet+}$ contributes significantly to the overall spin population, in contrast to the case of propylamine. By careful comparison of the spectra for propyl- and butylamine solutions at high concentration, it can be proved that the formation of the aminyl radicals $-CH_2N^{\bullet}H$ or $-CH_2N^{\bullet}D$ also occurs in the case of butylamines, and their contribution to the overall spin population can be estimated at about 50%.

As it can be reasonably assumed that clusters associated by hydrogen bonding would also be formed at the high butylamine concentration, our results indicate the competitiveness of the 1,5-hydrogen shift over the hydrogen/proton-transfer reaction in the hydrogen-bridged complex. At 125 K an iminyl radical can be observed (Figure 7c), with a set of coupling constants (*a*/G: 80.8 ($1H_\beta$), 9.9 (N_{iso}) and ~ 2.2 ($3H_{\gamma,\delta}$)) similar to the propane-1-iminyl radical, differing only in an additional, small 2 G splitting. We also note that after illumination of $\mathbf{6}^{\bullet+}$ with UV light ($\lambda \sim 350$ nm), small bands with a spacing of 175 G are observed outside the main spectrum; these bands indicate the formation of the methyleneiminyl radical $\mathbf{11}^{\bullet}$ at low concentration, as in the case of propylamine.

Kinetics of intramolecular hydrogen atom abstraction in case of *n*-propylamine: The transformation of the parent radical cation $\mathbf{1}^{\bullet+}$ into the distonic cation $\mathbf{2}^{\bullet+}$ was studied in the temperature range 130–145 K. The kinetics at 140 K as an example is given in Figure 8. The formation rate of $\mathbf{2}^{\bullet+}$ ($0.71\,h^{-1}$, measured with the amplitude of its main line, Figure 1d) and the decay rate of $\mathbf{1}^{\bullet+}$ ($0.66\,h^{-1}$, measured with its relatively noisy outer line, marked with an asterisk in Figure 1c) agree reasonably well. Further evidence for the 1:1 transformation is given by the constant total spin concentration. The transformation rate does not depend on the concentration and it is independent of deuteration at the NH_2 group. In the investigated temperature range, an apparent activation energy of $10.8\,kJ\,mol^{-1}$ can be derived for this hydrogen migration reaction (Figure 8, inset). However, if

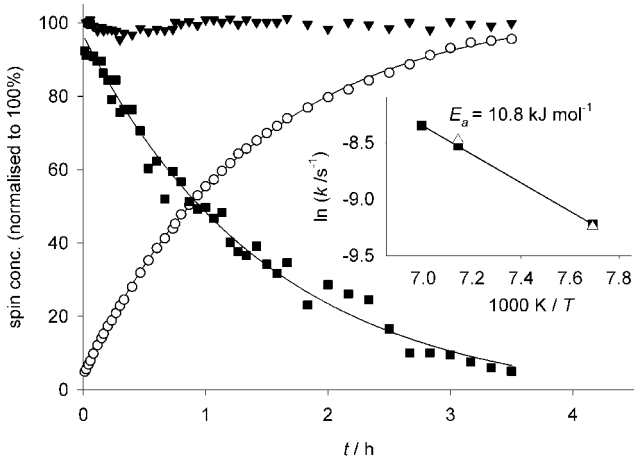

Figure 8. Time dependence of total spin concentration (▼) (normalised to 100%) and relative concentrations of species $\mathbf{1}^{\bullet+}$ (■) and $\mathbf{2}^{\bullet+}$ (○) as measured at 140 K. Inset: Arrhenius plot (of the apparent activation energy) for the transformation $\mathbf{1}^{\bullet+} \rightarrow \mathbf{2}^{\bullet+}$ for $PrNH_2$ (■) and $PrND_2$ (△).

quantum tunnelling contributes to the reaction rate, the activation energy may be much less than the true barrier height. Incidentally, it should be noted here that kinetic measurements taken over a narrow temperature interval[24] are unlikely to reveal the nonlinear Arrhenius plots that are symptomatic of hydrogen-atom tunnelling.[24c,26b–26d] For *n*-butylamine the transformation kinetics could not be studied quantitatively, as the reaction at 77 K is so fast that it is already complete one minute after irradiation.

As noted in the introduction to this paper, there is already much evidence from mass-spectrometric isotope-labelling studies[14e,g] that *n*-alkylamine radical cations in the gas phase can undergo facile 1,5-, 1,6- and 1,7-intramolecular hydrogen-atom abstraction reactions prior to NH_3 migration and fragmentation. Similarly, a 1,5-hydrogen transfer to an aminium radical cation is considered to represent the first step in the Hofmann–Löffler–Freytag synthesis of pyrrolidines.[12,13] However, in none of these studies has the hydrogen atom transfer reaction been isolated for kinetic study, and only estimates are available from such experiments for the barriers to these hydrogen shifts.[14f,15] In essence, the results of these previous investigations have established that 1,5- and more distant 1,*n*- ($n>5$) shifts are favoured over 1,4-shifts, and that 1,3- and 1,2-shifts are not generally observed.[14f] This conclusion is also in agreement with theoretical calculations,[15] showing that the barrier height increases by approximately 50 kJ mol^{-1} in going from a 1,5-shift in the *n*-butylamine radical cation to a 1,4-shift in the *n*-propylamine radical cation.

The present work is consistent with these previous findings, but adds significant quantitative information concerning the kinetics at low temperatures. Firstly, a low barrier to the 1,5-shift in the *n*-butylamine radical cation is indicated by the fact that the reaction already occurs within the short irradiation time of a few minutes at 77 K. The results of the calculations displayed in Figure 3 give a barrier of 13.5 kJ mol^{-1}, in reasonable agreement with the earlier estimate of 18 kJ mol^{-1}.[15] Secondly, in contrast to the ease of this 1,5-shift, the 1,4-shift in the *n*-propylamine radical cation is undetectable at 77 K, but can be observed directly over a period of hours after raising the temperature above 120 K. In this case the barrier height (Figure 3) is calculated to be 71.6 kJ mol^{-1}, which agrees closely with the 68 kJ mol^{-1} reported earlier.[15]

According to the theoretical calculations of Yates and Radom,[15] the rate constant at 298 K and the Arrhenius activation energy for this latter reaction are estimated to be 4.2×10^{1} s^{-1} and 57 kJ mol^{-1}, respectively. Using these values, which only incorporate the Wigner correction for the relatively small degree of tunnelling applicable at 298 K,[25a,b] the rate constants for the *n*-propylamine radical cation at 120 and 140 K are predicted to be 6.4×10^{-14} and 2.2×10^{-10} s^{-1}, respectively. These rate constants are much too small to account for our results. For example, the observed reaction half-life of around 1 h at 140 K corresponds to a rate constant of 1.93×10^{-4} s^{-1}, which is a factor of $\sim10^{6}$ larger than the theoretical value extrapolated from 298 K. Thus it seems likely that the tunnelling correction at 140 K is far larger than that (~360) suggested by the Wigner equation.[25a,b] In previous studies of hydrogen-atom abstraction reactions at cryogenic temperatures,[26] tunnelling corrections have ranged from 10^{5} to 10^{15},[25b] so it is not surprising that extensive tunnelling can augment the reaction rate for the *n*-propylamine radical cation at 140 K. This is entirely consistent with the fact that the apparent activation energy for the latter system of 10.8 kJ mol^{-1} is considerably lower than the calculated barrier height of around 70 kJ mol^{-1}.[27]

In contrast, the more rapid reaction for the *n*-butylamine radical cation at 77 K can be explained qualitatively without recourse to a large tunnelling "correction." Thus, an "over-the-barrier" estimate with a frequency factor of 1.5×10^{12} s^{-1} and an Arrhenius factor exp ($-E_a/RT$) of 1.4×10^{-11} based on a predicted barrier of around 16 kJ mol^{-1} (vide supra) gives a rate constant of 2.1×10^{1} s^{-1}, some three orders of magnitude above the observable lower limit of around 1×10^{-2} s^{-1}. However, since the actual rate constant could in fact be very much higher than this limit, a contribution from tunnelling cannot be ruled out.

Conclusion

In this work, direct evidence from low-temperature EPR studies has established the elementary reactions that constitute the pathways for the thermal and photoinduced rearrangements of the *n*-propylamine and *n*-butylamine radical cations. This has been achieved through the detailed assignment of the EPR spectra, corresponding to the initial and final signal carriers, and by monitoring the kinetics of the thermal transformation for the *n*-propylamine cation. In the case of the thermal reactions, the isolated single-reaction initial processes are shown to be the intramolecular 1,4- and 1,5-hydrogen shifts from carbon to nitrogen; these processes are of key mechanistic significance in the classical Hofmann–Löffler–Freytag reaction. The rates of these reactions are found to be in accordance with theoretical calculations that predict a much lower barrier for the 1,5-shift in the *n*-

butylamine radical cation than for the 1,4-shift in the *n*-propylamine radical cation. The fact that the apparent Arrhenius activation energy (10.8 kJ mol^{-1}) derived from the kinetic studies on the ionised *n*-propylamine over the narrow temperature range of 125–140 K is much lower than the barrier height predicted theoretically (ca. 60–70 kJ mol^{-1}) strongly suggests that a large contribution from quantum mechanical tunnelling becomes significant under these cryogenic conditions. The contribution from tunnelling in the case of the *n*-butylamine radical cation rearrangement at 77 K appears to be less significant in view of the much lower barrier height.

The photoinduced reactions of the primary *n*-propylamine radical cation **1**$^{\bullet+}$ also result in a 1,3-hydrogen shift, leading to the distonic radical cation **3**$^{\bullet+}$ with spin located at a secondary carbon atom. Although the latter is energetically the most stable $C_3H_9N^{\bullet+}$ isomer, its formation does not take place spontaneously (due to the barrier height of ~ 120 kJ mol^{-1}). It requires additional energy supplied by photoactivation.

Aminyl radicals -$CH_2N^{\bullet}H$ are formed in a deprotonation/hydrogen-abstraction reaction of the primary radical cations with a neutral molecule. This reaction is strongly enhanced under the condition of high solute concentration, when ground state dimers are easily formed by hydrogen bonding between the amine groups. It is worth noting that in case of *n*-butylamine, the intramolecular isomerisation still competes efficiently with the intermolecular hydrogen transfer in the hydrogen-bonded complex, due to the very low activation barrier (13.5 kJ mol^{-1}) of the former reaction. A rearrangement of the aminyl radicals to the more thermodynamically stable α-aminoalkyl radicals $RC^{\bullet}H{-}NH_2$ has not been observed under our conditions. Instead, the evidence suggests that aminyl radicals disproportionate, giving rise to propane-1-imine, which then serves as the immediate precursor for the formation of the propane-1-iminyl radical.

A surprising result of the present work is the formation of the methylene imino radical $H_2C{=}N^{\bullet}$ after photoexcitation and of alkyliminyl radicals $RCH{=}N^{\bullet}$ under matrix conditions that allow diffusion. In each case this highlights the great stability of $RCH{=}N^{\bullet}$ radicals due to a strong hyperconjugation between the C–H σ-orbital(s) and the nitrogen 2p orbital of the unpaired electron. Iminyl radicals are important reaction intermediates and, as in the present case, they are often detected under circumstances in which their formation would not normally be expected.[21e]

Experimental Section

Materials: *n*-Propylamine (98% +, Lancaster) was purified by distillation and *n*-butylamine (99%, Lancaster) was used as received. Derivatives of amines deuterated on amino groups were prepared from corresponding protiated compounds by hydrogen exchange with heavy water (99.5% according to NMR spectroscopy); the mixture of amine with excess of D_2O (10-fold in mol) was stirred for about 20 h at room temperature; the amine was then separated by distillation and the procedure was repeated. The content of the deuterated compound in the final reaction product of ≥98% was estimated by NMR spectroscopy. 1,1,1-Trifluorotrichloroethane (99%, Aldrich or Acros) was purified by passing it through a column filled with neutral Al_2O_3. 1,1,2-Trifluorotrichloroethane (Uvasol 99.9%, Merck) was used as supplied.

Sample preparation and irradiation: Amines were dissolved in freons at solute to solvent concentrations typically between 1:500 and 1:1000 and carefully degassed by the freeze–thaw technique. The solutions were irradiated in the dark at 77 K in liquid nitrogen with the electron beam of a Linac (Elektronika U-003, Thorium, Moscow). A dose of ≈10–15 kGy (irradiation time ca. 1 min) was sufficient to generate an easily observable concentration of paramagnetic species. Irradiated samples were protected from light and the first spectrum was taken as soon as possible (within about 2.5 min) after irradiation.

EPR spectroscopy: The measurements were performed by using a Bruker ESP 300e spectrometer (9.5 GHz, 100 kHz modulation) equipped with either a finger Dewar (77 K) or a variable-temperature control unit (ER 4121 VT, at ≥95 K). Spectra were recorded at a microwave power of 0.1 mW and a modulation amplitude of 0.05 or 0.1 mT.

Sample photobleaching: A tungsten lamp (250 W) and a Xenon lamp (XBO 1000 W, Osram) equipped with a water heat-filter and coloured glass filters were used for sample illumination at 77 K (outside the ESR cavity).

Spectra simulations: Isotropic and anisotropic spectra simulations were performed using the WinSim[28] and SimFonia (BRUKER®) software, respectively.

Computational methods: Quantum chemical calculations were performed by using density functional theory (DFT) hybrid B3LYP[29a,b] methods with the standard 6-31G(d) basis set as implemented in the Gaussian 98 program.[30] It was shown[31] that B3LYP and several other DFT functionals (which set the HF exchange equal to 20%) tend to delocalise spin for radical cation structures in which localisation of the unpaired electron is expected. Therefore, calculations with the BH&HLYP method,[29c] which utilises a larger fraction of the HF exchange (50%), were made for comparison. Both B3LYP and BH&HLYP methods produce qualitatively similar geometrical and electronical molecular parameters. However, the hfs constants calculated with B3LYP are in slightly better agreement with the experiment.

[1] K. Kimura, S. Katsumata, Y. Achiba, T. Yamazaki, S. Iwata, *Handbook of HeI Photoelectron Spectra of Fundamental Organic Molecules*, Japan Scientific Societies Press, Tokyo, **1981**, pp. 114–121.

[2] a) G. N. Lewis, D. Lipkin, *J. Am. Chem. Soc.* **1942**, *64*, 2801; b) G. E. Johnson, A. C. Albrecht, *J. Chem. Phys.* **1966**, *44*, 3162; c) J. Lin, K. Tsuji, F. Williams, *J. Chem. Phys.* **1967**, *46*, 4982.

[3] a) T. M. McKinney, D. H. Geske, *J. Am. Chem. Soc.* **1965**, *87*, 3013; b) F. Gerson, W. Huber, *Electron Spin Resonance Spectroscopy of Organic Radicals*, Wiley-VCH, Weinheim, **2003**, pp. 25–26, 196–197.

[4] a) R. S. Davidson, *Radiation Curing in Polymer Science and Technology, Vol. 3* (Eds.: J. P. Fouassier, J. F. Rabek), Elsevier Applied Science, Essex (UK), **1993**, p. 153; b) R. S. Davidson, A. A. Dias, D. R. Illsley, *J. Photochem. Photobiol. A* **1995**, *91*, 153.

[5] T. B. Cavitt, B. Phillips, C. K. Nguyen, C. E. Hoyle, S. Jönsson, K. Viswanathan, *Abstr. Pap. Am. Chem. Soc.* **2001**, *222*, 301-POLY.

[6] a) J. Nie, L. Å. Lindén, J. F. Rabek, J. Ekstrand, *Acta Odontol. Scand.* **1999**, *57*, 1; b) A. Wrzyszczynski, E. Adamczak, L. Å. Lindén, S. Morge, J. F. Rabek, *RadTech Eur. 95 Conf. Proc.* **1995**, 107.

[7] C. Decker, F. Morel, S. Jönsson, S. C. Clark, C. E. Hoyle, *Abstr. Pap. Am. Chem. Soc.* **1996**, *212*, 135-MSE.

[8] S. Jönsson, K. Viswanathan, C. E. Hoyle, S. C. Clark, C. Miller, F. Morel, C. Decker, *Nucl. Instrum. Methods Phys. Res. Sect. B* **1999**, *151*, 268.

[9] a) O. Brede, D. Beckert, C. Windolph, H. A. Gottinger, *J. Phys. Chem. A* **1998**, *102*, 1457; b) O. Brede, *Radiat. Phys. Chem.* **1997**, *49*, 39.

[10] a) A. Krantz, B. Kokel, Y. P. Sachdeva, J. Salach, K. Detmer, A. Claesson, C. Sahlberg in *Monoamine Oxidase: Structure, Function, and Altered Functions* (Eds.: T. P. Singer, R. W. von Korff, D. L. Murphy), Academic Press, New York, **1979**, p. 51; b) J. T. Simpson, A. Krantz, F. D. Lewis, B. Kokel, *J. Am. Chem. Soc.* **1982**, *104*, 7155;

c) R. B. Silverman, S. J. Hoffman, W. B. Catus, III, *J. Am. Chem. Soc.* **1980**, *102*, 7126; d) R. B. Silverman, *Acc. Chem. Res.* **1995**, *28*, 335; e) R. B. Silverman, *The Organic Chemistry of Enzyme-Catalyzed Reactions*, Academic Press, San Diego, **2000**, pp. 132–141.

[11] a) R. H. Abeles, A. L. Maycock, *Acc. Chem. Res.* **1976**, *9*, 313; b) R. P. Hanzlik, R. H. Tullman, *J. Am. Chem. Soc.* **1982**, *104*, 2048; c) R. H. Tullman, R. P. Hanzlik, *Drug Metab. Rev.* **1984**, *15*, 1163; d) T. L. Macdonald, K. Zirvi, L. T. Burka, P. Peyman, F. P. Guengerich, *J. Am. Chem. Soc.* **1982**, *104*, 2050; e) J.-M. Kim, M. A. Bogdan, P. S. Mariano, *J. Am. Chem. Soc.* **1993**, *115*, 10591; f) J.-M. Kim, S. E. Hoegy, P. S. Mariano, *J. Am. Chem. Soc.* **1995**, *117*, 100.

[12] a) Y. L. Chow, W. C. Danen, S. F. Nelsen, D. H. Rosenblatt, *Chem. Rev.* **1978**, *78*, 243; b) F. Williams, *J. Am. Chem. Soc.* **1962**, *84*, 2895; c) R. S. Neale, M. R. Walsh, *J. Am. Chem. Soc.* **1965**, *87*, 1255; d) M. M. Green, J. M. Moldowan, M. W. Armstrong, T. L. Thompson, K. J. Sprague, A. J. Hass, J. J. Artus, *J. Am. Chem. Soc.* **1976**, *98*, 849; e) G. Pandey, *Synlett* **1992**, *7*, 546.

[13] a) M. E. Wolff, *Chem. Rev.* **1963**, *63*, 55; b) P. Kovacic, M. K. Lowery, K. W. Field, *Chem. Rev.* **1970**, *70*, 639; c) E. J. Corey, W. R. Hertler, *J. Am. Chem. Soc.* **1960**, *82*, 1657; d) R. S. Neale, *Synthesis* **1973**, *1*, 1; e) W. Carruthers, *Some Modern Methods of Organic Synthesis*, Cambridge University Press, Cambridge, **1971**, pp. 173–178.

[14] a) S. Hammerum, *Tetrahedron Lett.* **1981**, *22*, 157; b) H. E. Audier, A. Milliet, J. P. Denhez, *Org. Mass Spectrom.* **1983**, *18*, 131; c) H. E. Audier, A. Milliet, G. Sozzi, J. P. Denhez, *Org. Mass Spectrom.* **1984**, *19*, 79; d) S. Hammerum, S. Ingemann, N. M. M. Nibbering, *Org. Mass Spectrom.* **1985**, *20*, 314; e) G. Sozzi, J. P. Denhez, H. E. Audier, T. Vulpius, S. Hammerum, *Tetrahedron Lett.* **1985**, *26*, 3407; f) C. Wesdemotis, P. O. Danis, R. Feng, J. Tso, F. W. McLafferty, *J. Am. Chem. Soc.* **1985**, *107*, 8059; g) H. E. Audier, G. Sozzi, J. P. Denhez, *Tetrahedron* **1986**, *42*, 1179; h) D. H. Parker, R. B. Bernstein, D. A. Lichtin, *J. Chem. Phys.* **1981**, *75*, 2577; i) T. I. Sølling, C. Kötting, A. H. Zewail, *J. Phys. Chem. A* **2003**, *107*, 10872.

[15] B. F. Yates, L. Radom, *J. Am. Chem. Soc.* **1987**, *109*, 2910.

[16] a) B. F. Yates, W. J. Bouma, L. Radom, *J. Am. Chem. Soc.* **1984**, *106*, 5805; b) B. F. Yates, W. J. Bouma, L. Radom, *Tetrahedron* **1986**, *42*, 6225; c) S. Hammerum, *Mass Spectrom. Rev.* **1988**, *7*, 123.

[17] F. Gerson, W. Huber, *Electron Spin Resonance Spectroscopy of Organic Radicals*, Wiley-VCH, Weinheim, **2003**, pp. 175–179.

[18] a) T. Cole, *J. Chem. Phys.* **1961**, *35*, 1169; b) A. J. Tench, *J. Chem. Phys.* **1963**, *38*, 593; c) M. C. R. Symons, *J. Chem. Soc. Perkin Trans. 2* **1973**, 797; d) G. W. Eastland, C. N. R. Rao, M. C. R. Symons, *J. Chem. Soc. Perkin Trans. 2* **1984**, 1551; e) V. N. Belevskii, O. I. Khvan, S. I. Belopushkin, V. I. Feldman, *Dokl. Akad. Nauk SSSR* **1985**, *281*, 869; f) G. W. Eastland, D. N. R. Rao, M. C. R. Symons, *J. Chem. Soc. Faraday Trans. 1* **1986**, *82*, 2833; g) X.-Z. Qin, T. C. Pentecost, J. T. Wang, F. Williams, *J. Chem. Soc. Chem. Commun.* **1987**, 450; h) A. de Meijere, V. Chaplinski, F. Gerson, P. Merstetter, E. Haselbach, *J. Org. Chem.* **1999**, *64*, 6951.

[19] K. S. Chen, P. J. Krusic, P. Meakin, J. K. Kochi, *J. Phys. Chem.* **1974**, *78*, 2014.

[20] a) B. W. Walther, F. Williams, *J. Chem. Phys.* **1983**, *79*, 3167; b) X.-Z. Qin, Q.-X. Guo, J. T. Wang, F. Williams, *J. Chem. Soc. Chem. Commun.* **1987**, 1553; c) F. Williams, X.-Z. Qin, *Radiat. Phys. Chem.* **1988**, *32*, 299.

[21] a) E. L. Cochran, F. J. Adrian, V. A. Bowers, *J. Chem. Phys.* **1962**, *36*, 1938; b) K. D. J. Root, M. C. R. Symons, *J. Chem. Soc. A* **1968**, 21; c) R. J. Egland, M. C. R. Symons, *J. Chem. Soc. A* **1970**, 1326; d) M. Kamachi, K. Kuwata, S. Murahashi, *J. Phys. Chem.* **1971**, *75*, 164; e) M. C. R. Symons, *Tetrahedron* **1973**, *29*, 615; f) P. H. Kasai, L. A. Eriksson, *Mol. Phys.* **1999**, *96*, 993.

[22] F. Gerson, W. Huber, *Electron Spin Resonance Spectroscopy of Organic Radicals*, Wiley-VCH, Weinheim, **2003**, pp. 54–55.

[23] a) X.-Z. Qin, F. Williams, *J. Am. Chem. Soc.* **1987**, *109*, 595; b) S. Dai, Q.-X. Guo, J. T. Wang, F. Williams, *J. Chem. Soc. Chem. Commun.* **1988**, 1069.

[24] a) E. D. Sprague, F. Williams, *J. Am. Chem. Soc.* **1971**, *93*, 787; b) R. J. Le Roy, E. D. Sprague, F. Williams, *J. Phys. Chem.* **1972**, *76*, 546; c) J.-T. Wang, F. Williams, *J. Am. Chem. Soc.* **1972**, *94*, 2930; d) W. Knolle, V. I. Feldman, I. Janovský, S. Naumov, R. Mehnert, H. Langguth, F. F. Sukhov, A. Yu. Orlov, *J. Chem. Soc. Perkin Trans. 2* **2002**, 687; e) M. Iwasaki, H. Muto, K. Toriyama, K. Nunome, *Chem. Phys. Lett.* **1984**, *105*, 586; f) J. Rideout, M. C. R. Symons, *J. Chem. Soc. Perkin Trans. 2* **1986**, 625; g) W. Knolle, I. Janovský, S. Naumov, R. Mehnert, *J. Chem. Soc. Perkin Trans. 2* **1999**, 2447; h) H. Tachikawa, N. Hokari, H. Yoshida, *Chem. Phys. Lett.* **1995**, *241*, 7.

[25] a) E. Wigner, *Z. Phys. Chem. Abt. B* **1932**, *19*, 203; b) R. P. Bell, *The Tunnel Effect in Chemistry*, Chapman and Hall, London, **1980**, p. 53, 108.

[26] a) R. J. Le Roy, H. Murai, F. Williams, *J. Am. Chem. Soc.* **1980**, *102*, 2325; b) R. L. Hudson, M. Shiotani, F. Williams, *Chem. Phys. Lett.* **1977**, *48*, 193; c) G. Brunton, D. Griller, L. R. C. Barclay, K. U. Ingold, *J. Am. Chem. Soc.* **1976**, *98*, 6803; d) G. Brunton, J. A. Gray, D. Griller, L. R. C. Barclay, K. U. Ingold, *J. Am. Chem. Soc.* **1978**, *100*, 4197; e) A. Campion, F. Williams, *J. Am. Chem. Soc.* **1972**, *94*, 7633.

[27] It should be clearly understood that the calculations are merely qualitative, since they do not take into account medium effects, which could be important, especially regarding the width of reaction barriers in solid matrices. Nevertheless, as the rate constants differ by less than a factor of two in the different freon matrices, the contribution of tunnelling, which is expected to be quite significant at these low temperatures, appears to be relatively insensitive to matrix effects. Therefore, any "discrepancy" between calculation and measurement can be attributed to both the simplified mathematical treatment and the need for a more rigorous theoretical description of the likely tunnelling mechanism for the hydrogen transfer at low temperatures.

[28] D. R. Duling, *J. Magn. Reson. Ser. B* **1994**, *104*, 105.

[29] a) A. D. Becke, *J. Chem. Phys.* **1993**, *98*, 5648; b) C. Lee, W. Yang, R. G. Parr, *Phys. Rev. B* **1988**, *37*, 785; c) A. D. Becke, *J. Chem. Phys.* **1996**, *104*, 1040.

[30] M. J. Frisch, G. W. Trucks, H. B. Schlegel, G. E. Scuseria, M. A. Robb, J. R. Cheeseman, V. G. Zakrzewski, J. A. Montgomery, Jr., R. E. Stratmann, J. C. Burant, S. Dapprich, J. M. Millam, A. D. Daniels, K. N. Kudin, M. C. Strain, O. Farkas, J. Tomasi, V. Barone, M. Cossi, R. Cammi, B. Mennucci, C. Pomelli, C. Adamo, S. Clifford, J. Ochterski, G. A. Petersson, P. Y. Ayala, Q. Cui, K. Morokuma, P. Salvador, J. J. Dannenberg, D. K. Malick, A. D. Rabuck, K. Raghavachari, J. B. Foresman, J. Cioslowski, J. V. Ortiz, A. G. Baboul, B. B. Stefanov, G. Liu, A. Liashenko, P. Piskorz, I. Komaromi, R. Gomperts, R. L. Martin, D. J. Fox, T. Keith, M. A. Al-Laham, C. Y. Peng, A. Nanayakkara, M. Challacombe, P. M. W. Gill, B. Johnson, W. Chen, M. W. Wong, J. L. Andres, C. Gonzalez, M. Head-Gordon, E. S. Replogle, J. A. Pople, Gaussian 98 (Revision A.11), Gaussian, Inc., Pittsburgh PA, **2001**.

[31] a) T. Bally, W. T. Borden, *Rev. Comput. Chem.* **1999**, *13*, 1; b) S. Naumov, I. Janovský, W. Knolle, R. Mehnert, *Nucl. Instrum. Methods Phys. Res. Sect. B* **2003**, *208*, 385.

Received: April 23, 2004
Published online: September 29, 2004